

# Microindentation studies on BaFCl single crystals

J. GUILLE

*IPCMS–GMI, EHICS, 1 rue Blaise Pascal, F-67008 Strasbourg Cedex, France*

M. SIESKIND

*Laboratoire PHASE, 23 rue du Loess, F-67037 Strasbourg Cedex, France*

The mechanical behaviour of BaFCl single crystals has been investigated by use of Vickers microindentation. The tests performed on (001) and (100) planes show an important hardness anisotropy, higher values being obtained on (100) planes and all being close to that of BaF<sub>2</sub>. A qualitative investigation of the impressions has established the occurrence of cleavage along {100} planes, whereas slip occurs much more easily along (001) planes. For tests performed on the (001) plane, a quantitative analysis of the indentation cracks yields a very low toughness value. On comparing the BaFCl and BaF<sub>2</sub> structures, it is concluded that the chlorine layers introduce a marked anisotropy but do not have the expected weakening effect.

## 1. Introduction

Barium fluorohalide compounds have been found to be very attractive materials for various applications, for example as spectroscopic and nuclear detectors [1–3]. A number of physical properties of these crystals are now available [4–8]. But surprisingly, information about their mechanical properties is very rare. The only data seem to be estimations of the elastic constants given by Balasubramanian *et al.* [9] and Sieskind and Ayadi [10] on the basis of optical measurements.

The indentation technique has been widely used to characterize the mechanical behaviour of brittle or semi-brittle crystals. Apart from its simplicity, it offers the advantage of being well adapted to small samples and allowing an investigation of their mechanical anisotropy. Studies were at first concerned with hardness anisotropy and deformation behaviour [11–14] and more recently, since Lawn and Wilshaw [15] and Evans and Charles [16] pointed out their interest, cracking phenomena arising around the impressions have been widely studied too (e.g. [17], [18]).

BaFCl has the layered PbFCl type of structure with the space group P4/nmm [19]. This structure is characterized by the packing of layers along the C<sub>4</sub> axis. The stacking is of the type: F–Ba–Cl–Cl–Ba–F . . . . Due to the weak bonding between the two chlorine layers, crystals are easily cleaved along the (001) plane and exhibit a strong mechanical anisotropy.

The goals of the present work are both to get an evaluation of the hardness of these crystals and to investigate the influence of crystalline anisotropy on the response to an indentation test.

## 2. Experimental procedure

### 2.1. Sample preparation

As previously described [4], single crystals of BaFCl were grown by cooling down a molten mixture of carefully dehydrated BaCl<sub>2</sub> and BaF<sub>2</sub> in a platinum boat placed in a quartz tube filled with argon gas. Typical crystal dimensions are 5 mm × 5 mm × 3 mm. These platelets are clear and colourless single crystals. Their orientation has been identified by X-ray diffraction techniques.

### 2.2. Indentation tests

Crystals were subjected to static indentation tests in air at room temperature using a Reichert microhardness tester fitted with a Vickers indenter. The indentation time was kept at 10 sec. Impression diagonals and crack lengths were measured with an optical microscope. Each result is an average value resulting from at least ten indentations. For crack measurements, only impressions yielding an acceptable crack pattern (four cracks of similar length) were taken into account. To make the crack length measurements easier and more precise, samples were slightly etched in dilute HCl after the tests were performed. This etching was confirmed to produce no change in crack length. Tests were performed on two different planes: (001), normal to the C<sub>4</sub> axis and (100), parallel to it.

## 3. Results

### 3.1. Tests on the (001) plane

The influence of the load and of the orientation of the indenter diagonals was investigated. Results are presented in two parts: the first is a qualitative description

of the deformation and fracture behaviour, and the second presents quantitative results.

### 3.1.1. Qualitative description

Tests were first performed in the 0.04 to 1 N load range, the indenter diagonals being parallel to  $\langle 100 \rangle$  directions. The main observations are the following:

- (i) Cracking occurs even for the smallest loads.
- (ii) Cracks are of two types: radial and lateral.
- (iii) Radial cracking occurs preferentially in  $(100)$  planes, the tendency being more pronounced for high loads.
- (iv) Lateral cracks remain most often in the sub-surface region, without emerging. Their presence is revealed by the interference fringes around the impressions. At the highest load level, they can emerge at the surface and produce intense chipping.

A second series of tests was performed on varying the orientation of the indenter diagonals. Surprisingly, no modification of the above-mentioned trends was noted and the crack patterns were very similar. An illustration of these observations is given in Fig. 1, in which several impressions corresponding to various load and orientation conditions can be seen. These observations were confirmed by SEM examination of the impressions, which gave two additional pieces of information:

- (i) The crystal surface is raised around the impression (Fig. 2). This can be due to both sub-surface lateral cracks and plastic deformation.
- (ii) Lines parallel to  $\langle 100 \rangle$  directions are visible in the central zone of the impression (Fig. 3). These lines probably result from the intersection of slip bands with the  $(001)$  plane. This observation is in good agreement with those made by Somaiah [20] concerning the presence of dislocations in planes intersecting the  $(001)$  plane along the  $\langle 100 \rangle$  directions.

### 3.1.2. Quantitative results

Results are presented in two sections: the first is concerned with the deformation behaviour, i.e. hardness results, and the second with the fracture behaviour.

**3.1.2.1. Hardness.** Only tests performed in the 0.08 to 0.8 N range were retained for hardness measurements. Hardness was calculated from the diagonal length  $d$  through the equation

$$H_V = 1854 Pd^{-2} \quad (\text{GPa})$$

where the load  $P$  is in Newtons and  $d$  in micrometres. Fig. 4 represents the hardness as a function of the test load. It first decreases with increasing load and is almost constant for loads above 0.25 N. This load dependence of microhardness is a classical although unexplained result. For brittle solids it is sometimes explained by the appearance and development of the cracks [21], but such an explanation is not fully satisfactory in this case as the cracks are well de-



Figure 1 Impressions, optical micrograph ( $\times 120$ ).

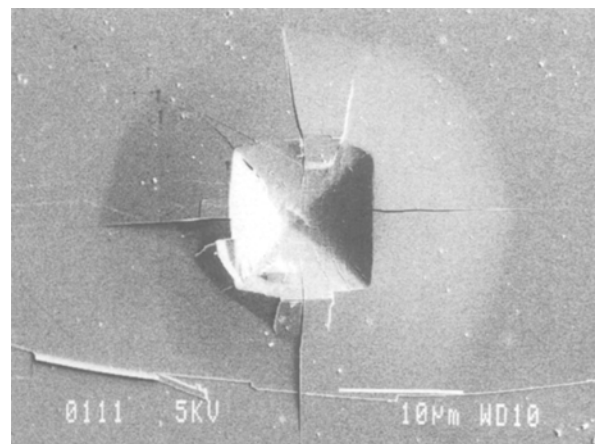


Figure 2 SEM micrograph: load 0.16 N, plane  $(001)$ , diagonals parallel to  $\{110\}$ .

veloped even for the smallest loads. Hardness was then measured at a constant 0.16 N load as a function of  $\theta$ , the angle between the  $\langle 100 \rangle$  directions and the indenter diagonals. Results are reported in Fig. 5. No appreciable hardness variation is detected.

**3.1.2.2. Fracture behaviour.** In the same manner as above, the crack length was studied as a function of load and indenter orientation. The load dependence of the crack length  $c$ , measured from the impression centre, is presented in Fig. 6 where  $\ln c$  is plotted

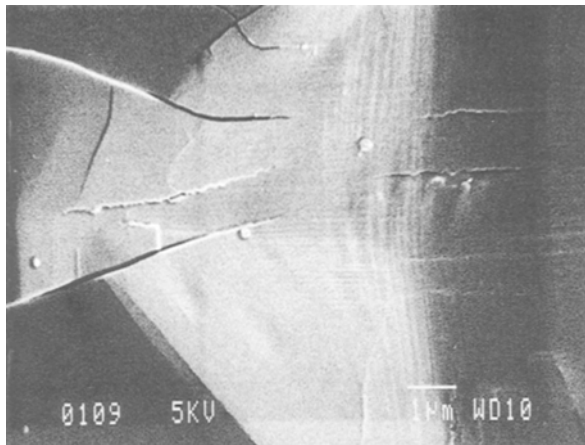


Figure 3 SEM micrograph: same conditions as Fig. 2 but diagonals parallel to {100}.

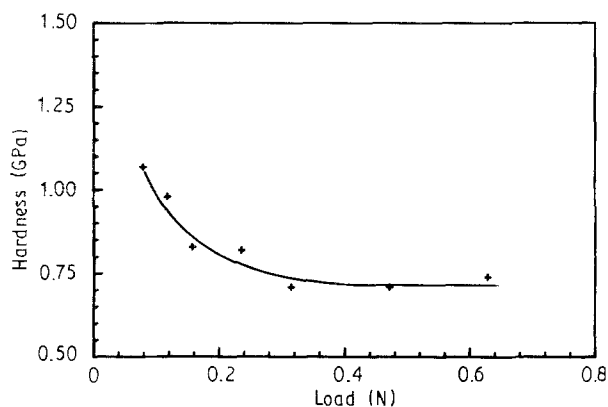


Figure 4 Vickers hardness as a function of load, (001) plane.

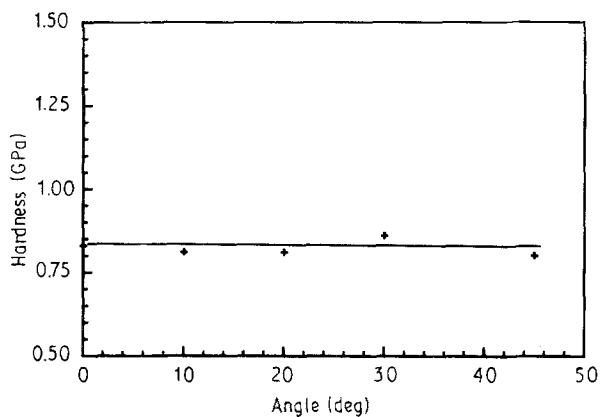


Figure 5 Vickers hardness as a function of the angle between the diagonal and the [100] direction.

against  $\ln P$ . The slope of this curve (0.63) is close to the theoretical value of 0.67 predicted by Lawn and Fuller [22]. This result, as well as the fact that the crack length to half-diagonal ratio is close to 3, allows us to consider the cracks as well-developed median cracks. It then becomes possible to evaluate the fracture toughness using one of the numerous equations proposed [21]. However, most of them require a value of Young's modulus or of the ratio of hardness to Young's modulus. In the absence of any value, the

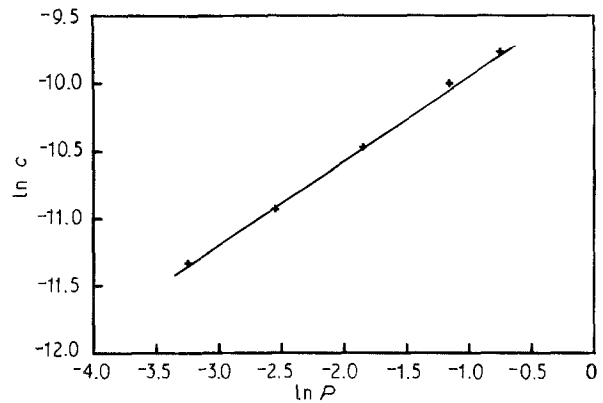


Figure 6 Evolution of the crack length against test load.

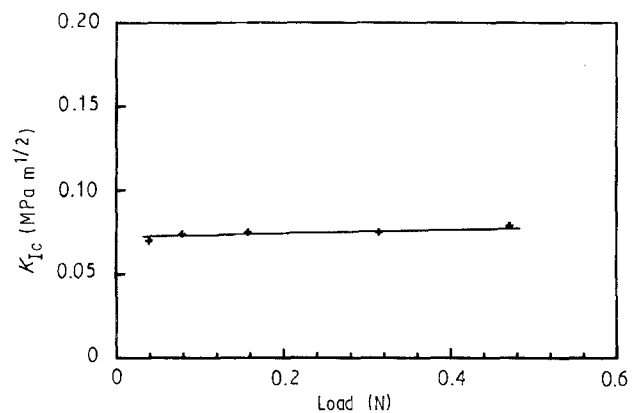


Figure 7 Evolution of the fracture toughness against test load.

equation proposed by Tanaka [23] has been used:

$$K_{Ic} = 0.0725 P - C^{-3/2} \quad (\text{MPa m}^{1/2})$$

The values obtained are plotted in Fig. 7 against load. It can be seen firstly that the variation is weak; and second, that even if these values must be considered as a first approximation they are very low.

### 3.2. Tests on the (100) plane

As above, the influence of the load and of the orientation was studied.

#### 3.2.1. Qualitative observations

In this case the phenomena are notably different depending on whether the indenter diagonals are parallel to the [100] and [001] directions or tilted at 45°. In the first case (Fig. 8), the impressions are no longer squares but lozenges, the [001] side being longer. In the second case, the impressions are rectangular, the larger side being once more parallel to [001]. More surprising is that in the first case, practically no cracks are observed in the [100] direction starting from the extremities of the [100] diagonal, but that lines parallel to [100] appear in the vicinity of the impressions. In the second case these lines are more numerous and intense chipping occurs.

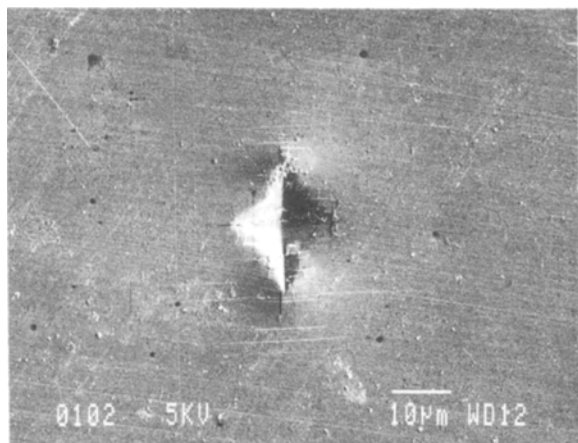


Figure 8 SEM micrograph: load 0.32 N, plane (100), diagonals parallel to [100] and [010].

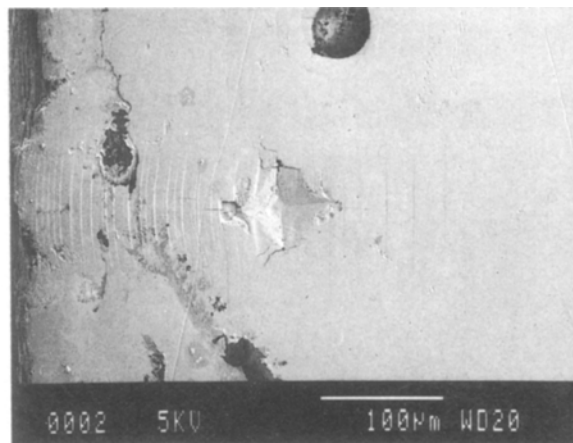


Figure 10 SEM micrograph: load 5 N (100) plane.

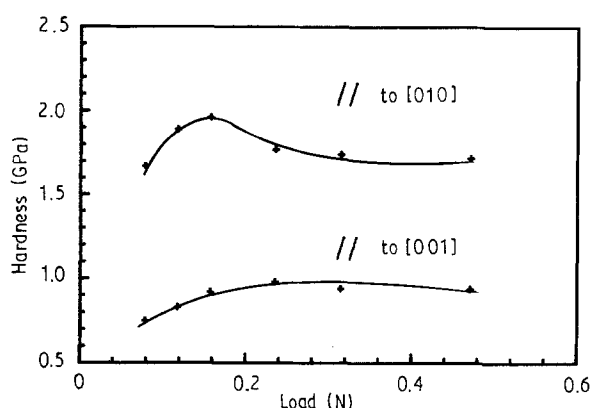


Figure 9 Vickers hardness as a function of load, (100) plane.

### 3.2.2. Hardness measurements

Only impressions of the first type were used to determine the hardness. Due to their anisotropy, two values were calculated, corresponding respectively to the [010] and [001] diagonals. Values are plotted against applied load in Fig. 9. In both cases, hardness first increases with increasing load; [100] hardness passes through a maximum and then slightly decreases, both remaining almost constant at loads above 0.2 N. The [100] value is always higher, the value of the  $H_{[100]}$  to  $H_{[001]}$  ratio being 1.8 in the 0.2 to 0.5 N range. This strong anisotropy proves that plastic deformation is much easier in the [001] than in the [100] direction. To get more information about the deformation and fracture behaviour, impressions were made using a substantially higher load (5 N), near a [100] edge of a (100) face of a crystal. SEM examination of these impressions allows additional observations (Fig. 10):

(i) Lines parallel to [100] most likely result from slipping in the (001) plane, as shown by the inversion on the two sides of the impression of the contrast associated with the lines.

(ii) In the region comprised between the impression and the crystal edge the lines are bent. This denotes the occurrence of plastic deformation which could result from the slip systems  $\{100\}\langle 001\rangle$ . This assumption is consistent with the presence mentioned

above (Section 3.1.1) of slip bands in the (001) plane, parallel to the  $\langle 100\rangle$  directions.

(iii) Cracks are preferentially parallel to [001] and result most probably from cleavage along (100) planes.

(iv) Chipping is caused by the intersection of cracks in the  $\{100\}$  and (001) planes.

## 4. Conclusions

The results obtained can be summarized as follows:

1. The hardness of BaFCl single crystals is comparable to that of  $RF_2$  compounds ( $R = Ca, Sr, Ba$ ) and close to that of  $BaF_2$  [12] but exhibits a strong anisotropy. As an example, for a 0.47 N test load

$$H_{(100)}/H_{(001)} = 1.79$$

in which  $H_{(100)}$  and  $H_{(001)}$  are the hardnesses measured respectively on the (100) and (001) faces, the latter being calculated from  $d = (d_{[100]} d_{[001]})^{1/2}$ .

2. Under Vickers indentation test conditions, cleavage occurs much more easily along (100) planes than along (001). The associated  $K_{Ic}$  value as evaluated from crack length measurements is very low.

3. Although not perfectly proved, the existence of the following slip systems may be assumed:  $\{100\}$  [001] and  $\{001\}$  [100].

4. The mechanical behaviour can be qualitatively described as follows:

Plane	Cleavage	Slip
$\{100\}$	Very easy	Possible
(001)	Rare	Very easy

These results suggest the following remarks. The structure of BaFCl presents some analogy with that of  $BaF_2$ . In both cases the fluorine ion has about it a tetrahedron of cations, and the distances between the two ions are almost the same. BaFCl may then be viewed as layers of such tetrahedra separated by two chlorine layers, the bidimensional arrangement of the tetrahedra being the same as in  $BaF_2$ . The interaction between barium and fluorine being the strongest in the crystal, this structural analogy may result in compar-

able hardness values. More surprising is that the presence of the chlorine layers seems to make the hardness increase. In particular, when the tests are performed on the (1 0 0) plane, smaller hardness values would be expected due to the easy gliding along the (0 0 1) planes, and the hardness is in fact higher. Concerning the fracture behaviour which is more strongly related to short-range forces, the results are surprising too. The expected and macroscopically observed easy cleavage along the (0 0 1) plane has not been observed around the impressions, although it can take place without breaking the strong Ba-F bonds. In contrast, (1 0 0) cleavage has been observed even at the smallest load level although it requires such bonds being broken.

The influence of the intermediate chlorine layers is thus not well understood. Enlightenment could be obtained by comparing these results with those which could be obtained with BaF<sub>2</sub> and BaF. In the first case there are no intermediate layers and the fracture behaviour is not known. In the second, the bonding between the BaF layers must be weaker.

## References

1. K. TAKAHASHI, J. MIYAHARA and Y. SHIBAHARA, *J. Electrochem. Soc.* **132** (1985) 1492.
2. M. SONODA, M. TAKANO, J. MIYAHARA and H. KATO, *Radiology* **148** (1983) 833.
3. B. HAMON, *Spectra 2000*, No. 112 (Vol. 14) (1986) 35.
4. M. SIESKIND, M. AYADI and G. ZACHMANN, *Phys. Status Solidi (b)* **136** (1986) 489.
5. K. INABE, S. NAKAMURA and N. TAKEUCHI, *ibid.* **149** (1988) K67.
6. Y. DOSSMANN, R. KUENZTLER, M. SIESKIND and D. AYACHOUR, *Solid State Commun.* **72** (1989) 377.
7. E. NICKLAUS, *Phys. Status Solidi (a)* **53** (1979) 217.
8. R. C. BAETZOLD, *J. Phys. Chem. Solids* **50** (1989) 915.
9. K. R. BALASUBRAMANIAN, T. M. HARIDASAN and N. KRISHNAMURTHY, *Chem. Phys. Lett.* **67** (1979) 530.
10. M. SIESKIND and M. AYADI, to be published.
11. C. A. BROOKES, J. B. O'NIELL and B. A. REDFERN, *Proc. R. Soc.* **A32** (1971) 73.
12. G. Y. CHIN, M. L. GREEN, L. G. VAN UITERT and W. A. HARGREAVES, *J. Mater. Sci.* **8** (1973) 1421.
13. G. R. SAWYER, P. M. SARGENT and T. F. PAGE, *ibid.* **15** (1980) 1001.
14. R. W. ARMSTRONG and C. C. WU, *J. Amer. Ceram. Soc.* **61** (1978) 102.
15. B. LAWN and T. R. WILSHAW, *J. Mater. Sci.* **10** (1975) 1049.
16. A. G. EVANS and E. A. CHARLES, *J. Amer. Ceram. Soc.* **59** (1976) 371.
17. J. L. HENSHALL and C. A. BROOKES, *J. Mater. Sci. Lett.* **4** (1985) 783.
18. D. Y. WATTS and A. F. W. WILLOUGHBY, *J. Mater. Sci.* **23** (1988) 272.
19. M. SAUVAGE, *Acta Crystallogr.* **B30** (1974) 2786.
20. K. SOMAIAH, *Cryst. Res. Technol.* **22** (1987) K141.
21. Z. LI, A. GHOSH, A. S. KOBAYASHI and R. C. BRADT, *J. Amer. Ceram. Soc.* **72** (1989) 904.
22. B. R. LAWN and E. R. FULLER, *J. Mater. Sci.* **10** (1975) 2016.
23. K. TANAKA, *ibid.* **22** (1987) 501.

*Received 2 February  
and accepted 19 February 1990*